Published in final edited form as:
*J Neuroimmunol*. 2015 February 15; 279: 64–70. doi:10.1016/j.jneuroim.2015.01.010.

# Microglial Content-Dependent Inhibitory Effects of Calcitonin Gene-Related Peptide (CGRP) on Murine Retroviral Infection of Glial Cells

**Jennifer Malon**[#a], **Eliza Grlickova-Duzevik**[#c], **James Vaughn**[a], **Holly Beaulac**[a], **Tyler R. Vunk**[b], and **Ling Cao**[a,*]

[a]Department of Biomedical Sciences, College of Osteopathic Medicine, University of New England, Biddeford, ME

[b]College of Arts and Sciences, University of New England, Biddeford, ME

[c]Graduate School of Biomedical Sciences and Engineering, University of Maine, Orono, ME.

[#] These authors contributed equally to this work.

## Abstract

C57BL/6 (B6) mice develop peripheral neuropathy post-LP-BM5 infection, a murine model of HIV-1 infection, along with the up-regulation of select spinal cord cytokines. We investigated if calcitonin gene-related peptide (CGRP) contributed to the development of peripheral neuropathy by stimulating glial responses. An increased expression of lumbar spinal cord CGRP was observed *in vivo*, post-LP-BM5 infection. Consequently, *in vitro* CGRP co-treatments led to a microglial content-dependent attenuation of viral loads in spinal cord mixed glia infected with selected doses of LP-BM5. This inhibition was neither caused by the loss of glia nor induced via the direct inhibition of LP-BM5 by CGRP.

### Keywords

Calcitonin gene-related peptide (CGRP); glia; LP-BM5; murine acquired immunodeficiency syndrome (MAIDS); retroviral infection; peripheral neuropathy

## 1. Introduction

As more effective antiretroviral therapies become available, human immunodeficiency virus (HIV)-1 infection is no longer represent a symbol of imminent death, but rather a chronic disease associated with a wide range of complications, including painful, HIV-associated



[*]Corresponding author: Ling Cao MD PhD, Department of Biomedical Sciences, College of Osteopathic Medicine, University of New England, 11 Hills Beach Road, Biddeford, ME 04005, USA, Tel: 1-207-602-2213, Fax: 1-207-602-5931, lcao@une.edu.

peripheral neuropathy (Cornblath and McArthur, 1988; Ellis et al., 2010; Hewitt et al., 1997; Miller, 1994; Simpson et al., 2002). Difficult to diagnose, HIV-associated peripheral neuropathy is often undertreated, which can, partially, be attributed to a lack of understanding of its pathophysiology (Cettomai et al., 2013; Cherry et al., 2005). Consequently, the FDA has not yet approved a treatment for HIV-associated peripheral neuropathy (Ellis et al., 2010).

In line with other studies, we have employed a murine retroviral isolate (LP-BM5) infection model to study HIV-1, as LP-BM5 induces a similar immunodeficiency syndrome (termed MAIDS) in susceptible C57BL/6 (B6) mice (Jolicoeur, 1991). Our current work has shown that B6 mice infected with LP-BM5 displayed behavioral and pathological signs of peripheral neuropathy, both of which were associated with tissue-specific cytokine expression, including the elevation of selected pro-inflammatory cytokines (such as IL-12) in the lumbar spinal cord, post-LP-BM5 infection (Cao et al., 2012).

Glial activation is a well-known contributor to HIV-associated neurological disorders (Kraft-Terry et al., 2009). Although few studies have explored the roles of glial cells in the development of HIV-associated peripheral neuropathy, animal studies have shown that spinal cord glial activation and the subsequent production of pro-inflammatory cytokines, can contribute to the development of HIV-1, gp120-induced sensory hypersensitivity (a behavioral sign of painful peripheral neuropathy) (Herzberg and Sagen, 2001; Milligan et al., 2000; Wallace et al., 2007; Zheng et al., 2011). As with HIV-1 in humans, the LP-BM5 virus can gain access to the central nervous system (CNS), leading to the direct infection of microglia and astrocytes (Sei et al., 1992). Upon viral stimulation, glia have been reported to produce pro-inflammatory cytokines and cytotoxic factors capable of contributing to LP-BM5-induced neuronal death and CNS symptoms (Kustova et al., 1998; Kustova et al., 1996; Suzumura et al., 1998).

Comprised of 37 amino acids, calcitonin gene-related peptide (CGRP) is a member of the calcitonin family and is predominantly produced by primary afferent neurons of small and medium diameters (Arulmani et al., 2004). Following peripheral nerve injury, these subsets of primary afferent neurons have been shown to increase both the release and expression of CGRP in the spinal cord (Gardell et al., 2003; Zheng et al., 2008). The administration of a $CGRP_{8-37}$, a CGRP antagonist, has been reported to reduce peripheral nerve injury-induced sensory hypersensitivity (Bennett et al., 2000; Lee and Kim, 2007). Furthermore, CGRP receptors have been detected on both microglia and astrocytes. We and others have previously reported on the CGRP-induced production of selected pro-inflammatory cytokines by glia (Malon et al., 2011; Moreno et al., 2002; Priller et al., 1995). Therefore, the current investigation was designed to elucidate the involvement of CGRP in LP-BM5-induced peripheral neuropathy, more specifically, the potential influence of CGRP-induced glial responses in LP-BM5-induced peripheral neuropathy.

## 2. Materials and Methods

### 2.1 Mice

Adult (7 wks old) male C57BL/6 (B6) mice were purchased from the National Cancer Institute (NCI, Frederick, MD) and were allowed to habituate to the animal facility at the University of New England (UNE, Biddeford, ME) for a minimum of one week prior to experimentation. All mice were group-housed with food and water *ad libitum* and maintained on a 12-hour light/dark cycle. The Institutional Animal Care and Use Committee at UNE approved all of the experimental procedures for this study.

### 2.2 LP-BM5 virus

LP-BM5 viral stock was initially obtained from Dr. William R. Green, Geisel School of Medicine at Dartmouth College (Hanover, NH). The viral stock was propagated and maintained in our laboratory as previously described (Cao et al., 2012). Aliquots of the viral stock were quantified using a previously reported XC plaque assay (Rowe et al., 1970) and stored at −80°C. For all *in vivo* studies, LP-BM5 was given intraperitoneally (i.p.) at $5 \times 10^4$ plaque-forming units (PFU) per mouse.

### 2.3 CGRP immunohistochemistry (IHC)

Fluorescent IHC for CGRP was conducted following our previously published method using a rabbit anti-CGRP primary Ab (1:5,000, Sigma-Aldrich, St. Louis, MO) and a Cy3-anti rabbit IgG secondary Ab (1:800, Jackson ImmunoResearch Laboratories, West Grove, PA) (Malon et al., 2011). Prior methods were also employed to determine the CGRP expression in spinal cord dorsal horn slices (Malon et al., 2011). Total dorsal horn and $CGRP^+$ areas were defined and measured for each L5 dorsal horn image and then the relative CGRP expression was calculated as follows: $CGRP^+$ area/total dorsal horn area. For each sample, at least three tissue slices were analyzed and the average expression of these slices was calculated. All images were analyzed by persons blinded to the treatment groups.

### 2.4 Primary adult mixed glia culture and treatment

Primary adult mixed glia cultures were established using 8-week-old B6 mice and maintained in complete Dulbecco's Modified Eagle Media (cDMEM) (Lonza, Walkersville, MD) containing 50 μM 2-mercaptoethanol (2-ME, Sigma-Aldrich) in 12-well plates as we have previously described (Malon et al., 2011). Media was replaced on days 2, 4, 8, and 12 after the establishment of each culture. All cells were maintained at 37°C, in a humidified atmosphere with 5% $CO_2$. Later, in order to obtain mixed glial cultures with higher microglial content, we followed a previously published method and incubated primary glia at 36°C until treatment (data in Figures 3 and 4; see below for detail) (Mayer et al., 2001).

Primary mixed glial cells were considered ready for treatment at 14 days after the establishment of the culture. Prior to treatment, the following were performed on each culture set: 1). Supernatants were collected and stored at −20°C for baseline cytokine measurements; 2). The average number of viable cells per well was determined by harvesting cells from several representative culture wells followed by enumeration with a hemocytometer using trypan blue exclusion stain (Sigma-Aldrich). The average number of

cells per well for all experiments (at 37°C and 36°C) was 94,045 ± 10,772 (mean ± SEM) per well. No significant differences in the total cell number per well were observed when cells were cultured at 36°C vs. 37°C. Additionally, the microglial content within cells collected ((2) above) was analyzed via flow cytometry using monoclonal antibodies (mAbs) against CD45 and CD11b (eBiosciences, San Diego, CA) as previously described (Malon et al., 2011). The $CD45^{lo}CD11b^{+}$ population was identified as microglia. Mixed glia cultured at 37°C had an average microglial content of 9.28% ± 2.08 whereas mixed glia cultured at 36°C had an average microglial content of 26.23% ± 7.15.

Virus stock for the LP-BM5 infection was serially diluted in sterile, phosphate-buffered saline (PBS) containing 0.1μg/μl polybrene (Sigma-Aldrich) to promote the binding of the virus to target cells. After media removal, cells were inoculated with 100 μl/well of diluted virus. The final concentrations of LP-BM5/well were 0, $10^1$, $10^2$, and $10^3$ (PFU). All plates were then incubated for 1 hour at 37°C, with gentle rocking every 15 minutes to ensure an equal distribution of virus-containing solutions. In separate pilot experiments, we determined (via XC plaque assay, see below) that the amount of viable virus showed no significant change for at least 4 hours when incubated in PBS alone. Following incubation, 900 μl of cDMEM containing 2-ME, both with and without 1,000 ng/ml of CGRP (Alpha Diagnostic, San Antonio, TX), were added to selected culture wells. The dose of CGRP was selected based upon both observations from our previous study regarding CGRP's effects on mixed glia (Malon et al., 2011) and our pilot experiments involving infected glia.

Media was changed on days 1 and 4, post-infection. Briefly, plates were centrifuged at 281 g for 5 minutes (4°C). Half of the supernatant (500 μl) was then collected from each well and stored at −20°C until cytokine/chemokine analyses were performed. Each well was replenished with 500 μl of fresh media. Depending upon the experiment (single CGRP treatment vs. repeated CGRP treatment), wells treated with CGRP received fresh media either with, or without CGRP (at 1,000 ng/well). On day 7, post-infection, supernatants from each well were collected as described above, and cells were harvested through trypsinization. Cells were then lysed in a single freeze and thaw cycle. Cell lysates were collected and used for plaque assay (see below).

### 2.5 XC Plaque Assay

XC plaque assays were performed using a protocol adapted from Rowe et. al 1970 (Rowe et al., 1970). Briefly, cDMEM-suspended SC-1 cells (American Type Culture Collection (ATCC) Manassas, VA) were seeded into 6-well plates (VWR, Bridgeport, NJ) at a concentration of 200,000 cells/4 ml/well. Plates were incubated overnight at 37°C with 5% $CO_2$. The following day, SC-1 cells were washed with PBS and 500 μl of individual serially diluted samples (glial cell lysates in section 2.4, or viral suspension in section 3.4, diluted in PBS containing polybrene at 0.0024 μg/μl) were added to each well. Virus stock was used as a positive control and PBS/Polybrene solution was used as a negative control. Plates were then incubated and manually rocked every 15 minutes for 1 hour at 37°C with 5% $CO_2$. Seven ml of cDMEM were then added to each well, and plates were incubated at 37°C with 5% $CO_2$. Four days later, media were removed and plates were placed approximately 10 cm from an ultra-violet (UV) light source and exposed to UV light for 25 seconds. Following

irradiation, $1 \times 10^6$ XC cells (ATCC) suspended in 4 ml of cDMEM were added to each well. Plates were incubated at 37°C with 5% $CO_2$ for 3 additional days. XC cells were then fixed with 2 ml methanol (Fisher, Pittsburg, PA) and stained with 2 ml of 2% methylene blue (VWR) at room temperature for 30 minutes. Excess methylene blue was gently washed with tap water and plaques appeared as unstained areas in each well. Plaques were counted and viral concentrations were calculated.

### 2.6 RNA isolation and real-time quantitative RT-PCR (qRT-PCR) for viral load

Cell pellets were collected at the end of each experiment and stored at −80°C until viral load was quantified. LP-BM5 is a retroviral mixture that contains mainly a pathogenic, yet replication-defective virus (BM5def), and a non-pathogenic helper virus (ecotropic (mouse tropic) retrovirus (BM5eco)) (Chattopadhyay et al., 1989). Cellular viral load was determined by evaluating the expression of both BM5def and BM5eco gag RNAs via qRT-PCR, as previously described (Cao et al., 2012; Cook et al., 2003; Giese et al., 1994). Briefly, total RNA was isolated via the RNeasy kit (Qiagen, Valencia, CA). cDNA was synthesized with the iScript cDNA Synthesis kit (Bio-Rad, Hercules, CA) from 0.5 μg of total RNA, and qRT-PCR was performed by amplifying the cDNA (1 μl) with the SYBR Green Supermix (Bio-Rad) on an iCycler with iCycler iQ software (Bio-Rad). Mouse β-actin RNA expression was measured in parallel. The relative expression levels of the BM5def gag and BM5eco gag genes were calculated via the ΔΔCt method using β-actin expression as the control. In each experiment, 2-3 wells of cells were pooled for RNA extraction and the subsequent qRT-PCR. Experiments were replicated several times for statistical analysis. Due to the variation between experiments and in order to make fair comparisons, within each experiment, the viral level of LP-BM5-treated group was set at 100% and viral levels for all other groups were normalized to the LP-BM5-treated group.

### 2.7 MTT assay

Following the various treatments described above, an MTT (3-(4,5-dimethylthiazol-2-yl)-2,5-diphenyltetrazolium bromide) assay (Sigma-Aldrich) was used to determine cell viability. The assay was performed according to the manufacturer's guidelines. Due to the variation between experiments and in order to make fair comparisons, within each experiment, the OD570 values of the non-treated control group (PBS) was set at 100% and the OD570 values for all other groups were normalized to the PBS control group.

### 2.8 Enzyme-linked immunosorbent assay (ELISA)

ELISAs for mouse cytokines/chemokines: IL-1β, IL-6, IL-12/IL-23 p40, TNFα, INFγ (R&D Systems, Minneapolis, MN), and CCL2 (BD Biosciences, San Jose, CA) were performed using detection kits in accordance with the manufacturer's protocols. The standard series ranged as follows: 0-1,000 pg/ml for IL-1β, IL-6, IL-12/IL-23 p40, and CCL2; 0-2,000 pg/ml for TNFα and INFγ.

### 2.9 Statistical analysis

All graphs were generated using SigmaPlot (Systat Software, Inc.) and all statistical analyses were performed with SigmaStat 3.5 software (Systat Software, Inc.). When

multiple groups were compared, appropriate analyses of variance (ANOVA) were performed followed by Student-Newman-Keuls (SNK) *Post hoc* analysis. The linear regression curve was generated using SigmaPlot and analysis of correlation was performed via SigmaStat3.5 linear regression analysis. All data are presented as mean ± SEM, and $p < 0.05$ was considered statistically significant.

## 3. Results

### 3.1 LP-BM5-induced lumbar spinal cord CGRP expression

Previously, we have shown that LP-BM5 infection induces peripheral neuropathy and that mice infected with LP-BM5 display neuropathic pain-like behaviors, i.e. increased hind paw sensitivities to mechanical and heat stimulations (Cao et al., 2012). Due to the pro-nociceptive effects of CGRP found in other animal models of neuropathic pain (Arulmani et al., 2004; Bennett et al., 2000; Gardell et al., 2003; Lee and Kim, 2007; Zheng et al., 2008), we examined CGRP expression in the lumbar spinal cord following LP-BM5 infection via a time course study (Figure 1). As previously described, relative CGRP expression was indicated by the ratio between the $CGRP^+$ area within the dorsal horn and the total dorsal horn area. Since no significant difference in CGRP expression between the left and right side of the spinal cord dorsal horn was observed (paired *t*-test, $p = 0.572$), further comparison was performed using two-way ANOVA factoring time and infection. It was found that LP-BM5 induced a significant increase of CGRP expression from 8 to 12 weeks, post-infection, when compared to non-infected mice (Figure 1B, two way ANOVA, $p_{time} = 0.020$, $p_{infection} = 0.001$ and $p_{timexinfection} = 0.218$).

### 3.2 CGRP induced glial responses post-LP-BM5 infection *in vitro*

We hypothesized that CGRP could stimulate spinal cord glial responses, such as proinflammatory responses, that then contribute to the development of peripheral neuropathy via central sensitization. Therefore, we evaluated the effects of CGRP on glial cell responses to LP-BM5 infection, *in vitro*. Glial cells were treated with CGRP either once or repeatedly, as described in the Materials and Methods. Interestingly, with both treatment regimens, when glial cells were treated with a selected dose of LP-BM5 (10 PFU for single CGRP treatment and 100 PFU for repeated CGRP treatment; these doses were used for later experiments), lower viral loads were detected in CGRP-treated glial cells compared to cells that were not treated with CGRP (Figure 2A and B), suggesting a potential viral inhibitory effect by CGRP. Further analysis indicated that CGRP's inhibitory effect is dependent upon the content of microglia within the mixed glial cells at the time of infection, i.e. CGRP exhibited a greater viral inhibitory effect when microglial content was increased. This effect is particularly significant when repeated CGRP treatments were used (Figure 2C, analysis of correlation indicates $p = 0.004$). According to the regression curve, CGRP's inhibitory effect is most evident when microglial content is above ~5%. Thus we defined mixed glial cultures that had greater than 5% of microglia as microglia-rich cultures and thoes had less than 2% of microglia as microglia-poor cultures.

From the same above experiments, supernatants were collected at days 1, 4, and 7 post-infection and their contained pro-inflammatory cytokines/chemokines: IL-1β, IL-6, TNFα,

IL-12/IL-23 p40, INFγ and CCL2 were measured via ELISAs. Both IL-1β and IFNγ levels were too low to detect. With regard to the remaining cytokines/chemokines, there was a general increase in cytokine/chemokine production with time; however, no significant treatment effects (via LP-BM5 or CGRP) were detected at any of the collection times. Representative cytokine/chemokine data are shown in Table 1.

To further confirm CGRP's viral-reducing effect in mixed glial cells, we performed similar experiments with repeated CGRP treatment and quantified viral loads using another method, qRT-PCR. Since CGRP's effect was microglial-content dependent, we prepared additional sets of mixed glial cultures that were microglia-rich (see Materials and Methods for more detail). Consistent with the results obtained from the plaque assay (Figure 2B), when microglial content was greater than 5% at the time of treatment (5% was chosen based on the regression curve in Figure 2C), we observed that CGRP significantly reduced the levels of BM5def RNA at day 7 post-treatment (Figure 3A, one-way ANOVA, $p < 0.001$ and $p < 0.05$ LP-BM5 vs. LP-BM5+CGRP group). Levels of BM5 eco were also reduced with CGRP treatment, however, they did not reach statistical significance (Figure 3B, one-way ANOVA, $p = 0.03$). When microglial content was less than 2% at the time of treatment (microglia-lacking), as suggested by the results in Figure 2, CGRP did not significantly reduce the viral loads in mixed glia (Figure 3C and D). Instead, it appears that CGRP increased the RNA levels of both BM5def and BM5eco (Figure 3C, one-way ANOVA, $p = 0.022$; Figure 3D, one-way ANOVA, $p = 0.034$). Altogether, our data showed that CGRP significantly reduced LP-BM5 viral levels in mixed glia when microglial content is relatively high (> 5%).

### 3.3 Effects of CGRP on glial cell viability post-LP-BM5 infection

To determine whether CGRP induced the reduction of viral loads within mixed glial cells via the promotion of glial cell death upon-infection, we tested the viability of microglia-rich mixed glial cells that were treated with LP-BM5 ± CGRP via MTT assay. CGRP did not significantly change the cell viability of infected mixed glial cells (Figure 4). Thus, CGRP does not reduce viral load within mixed glia by reducing the numbers of host cells.

### 3.4. Direct effects of CGRP on LP-BM5 virus

We also tested whether CGRP had a direct effect on viral viability in a cell-free environment. Viral particles were suspended in PBS ($10^4$ PFU/ml) containing varying concentrations of CGRP (0-10,000 ng/ml) and incubated at 37°C for 1 hour. At the end of the incubation, all viral suspensions were collected and subjected to the XC plaque assay for the determination of their viral content. All samples showed similar levels of virus, indicating that CGRP did not directly inhibit the survival, or replication of LP-BM5 virus that is not associated with host cells (Figure 5).

## 4. Discussion

Often accompanied by pain, HIV-associated peripheral neuropathy is the most common neurological disorder linked to HIV-1 infection. Yet, the mechanisms responsible for this complication are still poorly understood (Cornblath and McArthur, 1988; Ellis et al., 2010).

Previously, we have shown that B6 mice infected with LP-BM5 display sensory hypersensitivity (indicative of painful peripheral neuropathy), along with the development of peripheral immunodeficiency (Cao et al., 2012). It has been shown that administration of a CGRP antagonist can reduce peripheral nerve injury-induced sensory hypersensitivity, indicating a pro-nociceptive role for CGRP (Bennett et al., 2000; Lee and Kim, 2007). To help elucidate the pathophysiology of retroviral infection-induced painful neuropathy, we investigated the role of spinal cord CGRP during LP-BM5 infection. Similar to the observations made in some models of nerve injury-induced neuropathic pain, our study found that the LP-BM5 infection induced an increased expression of CGRP in the lumbar spinal cord dorsal horn. As this increase can be correlated to the development of previously-observed, LP-BM5-induced neuropathic pain-like behaviors, we evaluated whether or not CGRP's pro-nociceptive role is mediated by stimulating spinal cord glial responses, particularly cytokine production.

Our study revealed the surprising and exciting result that infected mixed glial cells treated with CGRP showed reduced viral loads. Cell viability tests and direct incubation of CGRP with LP-BM5 in a cell-free environment indicate that this reduction of viral load was not due to significant death of host cells upon infection, or due to the direct killing of LP-BM5 by CGRP. Thus our data suggest a potential anti-retroviral effect for CGRP upon its interaction with the host cells. Further investigation may lead to novel anti-retroviral therapies, which could be particularly beneficial to the development of new anti-HIV-1 treatments. Consistent with our findings, a recent report indicated an inhibitory role of CGRP in Langerhans cell-mediated HIV-1 transmission (Ganor et al., 2013). Since our study suggests that CGRP does not directly kill the virus, future studies will focus on CGRP's effects on host cells, as well as the interactions between the host cells and the virus. Of particular interest, murine cationic amino acid 1 (mCAT-1) is an established host cell receptor for LP-BM5 (Albritton et al., 1989; Wang et al., 1991). N-linked glycosylation of the virus binding domain within mCAT-1 and the subsequent conformational changes of mCAT-1 have been associated with increased resistance to LP-BM5 infection (Eiden et al., 1994; Wang et al., 1996). CGRP may reduce the susceptibility of glia to the LP-BM5 virus by modifying the levels of glycosylation of mCAT-1. Furthermore, CGRP may reduce LP-BM5 viral replication through the activation of several intracellular signaling pathways. It is known that CGRP conveys signals through CLR/RAMP1 receptors located in the cell membrane of glia (Eftekhari et al., 2010). Activation of CGRP receptors results in elevated cAMP levels and activation of protein kinase-A (PKA)-mediated pathways. Elevated levels of cAMP have been associated with halted HIV-1 viral transcription in T cells and dendritic cells (Moreno-Fernandez et al., 2012). CGRP has also been shown to signal through the NF-kB pathway and selected mitogen-activated protein kinase (MAPK) pathways (Millet et al., 2000; Parameswaran et al., 2000; Zhang et al., 2006). Activation of both the PKA and NF-kB pathways is thought to be involved in CGRP-induced inhibition of HIV-1 transmission via Langerhans cells (Ganor et al., 2013). MAPK pathways have also been implicated in HIV replication (Cohen et al., 1997; Emori et al., 2004; Zybarth et al., 1999). Particularly, p38 MAPK-mediated phosphorylation of heat shock protein (hsp) 27 has been shown to interfere with HIV-1 replication by inhibiting the HIV-1 viral protein R (Vpr)-induced cell arrest (Liang, 2007). Thus, further examinations of these pathways using the LP-BM5 model

may assist in the delineation of CGRP's role in retroviral infection and its possible therapeutic functions against retrovirus, such as HIV-1 infection.

Interestingly enough, CGRP's anti-retroviral effect in glia is dependent upon the microglial content. This is important because microglia are known to be associated with many neurological disorders, including HIV-associated neurological disorders (Kraft-Terry et al., 2009). Microglia can serve as an HIV-reservoir for infected individuals (Kramer-Hammerle et al., 2005). Similarly, microglia are thought to both harbor and help spread the LP-BM5 virus in the CNS of LP-BM5-infected B6 mice (Sei et al., 1998). Further investigation of CGRP's anti-retroviral effect could offer an anti-retroviral treatment that is specifically targeting microglia. Additionally, it is known that besides microglia, both HIV and LP-BM5 can infect astrocytes (Narasipura et al., 2014; Ojeda et al., 2014; Sei et al., 1998). The observed microglia-dependent effects may indicate differential CGRP-induced signaling pathways among microglia and astrocytes. The potential unique interactions between microglia and astrocytes during retroviral infection may exist as well. A recent study reported that, upon CNS simian immunodeficiency virus infection, astrocyte-producing chemokine CCL2 can regulate macrophage expression of anti-viral cytokines, such as IFNα, IFNβ, and their related genes (Zaritsky et al., 2012). As we did not observe significant CGRP-induced changes in the production of selected cytokines/chemokines by glia, CGRP's anti-retroviral effects are less likely to involve glial cytokines/chemokines. However, it is possible that CGRP exerts its effects on glial cells by regulating the expression and function of cytokine/chemokine receptors. Similar regulation by CGRP has been observed in dendritic cells (Mikami et al., 2014).

In conclusion, our data demonstrated that the LP-BM5 infection induced a significant, elevated expression of CGRP within the lumbar region of murine spinal cords, *in vivo*. This elevation may serve as a protective mechanism against an LP-BM5 viral infection within the CNS. CGRP's anti-retroviral effects are not due to its direct toxicity to host glial cells or LP-BM5 virus. Further investigations of CGRP's anti-retroviral effects are necessary, as their results might benefit the development of novel anti-retroviral treatments for HIV-related neurological disorders.

## Acknowledgements

The authors would like to thank Dr. William R. Green, Geisel School of Medicine at Dartmouth College, for providing the LP-BM5 viral stock and technical assistance with the establishment of viral stock in our laboratory and the XC plaque assay. The authors would also like to acknowledge Dr. Alejandro MS Mayer, Department of Pharmacology, Chicago College of Osteopathic Medicine for technical help with obtaining microglia-rich mixed glial cells. Funding for this project is provided by the NIH awards 5R21NS066130 (Cao) and P20GM103643 (Meng).

## References

Albritton LM, Tseng L, Scadden D, Cunningham JM. A putative murine ecotropic retrovirus receptor gene encodes a multiple membrane-spanning protein and confers susceptibility to virus infection. Cell. 1989; 57:659–666. [PubMed: 2541919]

Arulmani U, MaassenVanDenBrink A, Villalón CM, Saxena PR. Calcitonin gene-related peptide and its role in migraine pathophysiology. European Journal of Pharmacology. 2004; 500:315–330. [PubMed: 15464043]

Bennett AD, Chastain KM, Hulsebosch CE. Alleviation of mechanical and thermal allodynia by CGRP8-37 in a rodent model of chronic central pain. Pain. 2000; 86:163–175. [PubMed: 10779673]

Cao L, Butler MB, Tan L, Draleau KS, Koh WY. Murine immunodeficiency virus-induced peripheral neuropathy and the associated cytokine responses. J Immunol. 2012; 189:3724–3733. [PubMed: 22956581]

Cettomai D, Kwasa JK, Birbeck GL, Price RW, Cohen CR, Bukusi EA, Kendi C, Meyer AC. Screening for HIV-associated peripheral neuropathy in resource-limited settings. Muscle Nerve. 2013; 48:516–524. [PubMed: 24037693]

Chattopadhyay SK, Morse HC, Makino M, Ruscetti SK, Hartley JW. Defective Virus is Associated with Induction of Murine Retrovirus-Induced Immunodeficiency Syndrome. Proceedings of the National Academy of Sciences. 1989; 86:3862–3866.

Cherry CL, Wesselingh SL, Lal L, McArthur JC. Evaluation of a clinical screening tool for HIV-associated sensory neuropathies. Neurology. 2005; 65:1778–1781. [PubMed: 16344522]

Cohen PS, Schmidtmayerova H, Dennis J, Dubrovsky L, Sherry B, Wang H, Bukrinsky M, Tracey KJ. The critical role of p38 MAP kinase in T cell HIV-1 replication. Mol Med. 1997; 3:339–346. [PubMed: 9205949]

Cook WJ, Green KA, Obar JJ, Green WR. Quantitative analysis of LP-BM5 murine leukemia retrovirus RNA using real-time RT-PCR. J Virol Methods. 2003; 108:49–58. [PubMed: 12565153]

Cornblath DR, McArthur JC. Predominantly sensory neuropathy in patients with AIDS and AIDS-related complex. Neurology. 1988; 38:794–796. [PubMed: 2834669]

Eftekhari S, Salvatore CA, Calamari A, Kane SA, Tajti J, Edvinsson L. Differential distribution of calcitonin gene-related peptide and its receptor components in the human trigeminal ganglion. Neuroscience. 2010; 169:683–696. [PubMed: 20472035]

Eiden MV, Farrell K, Wilson CA. Glycosylation-dependent inactivation of the ecotropic murine leukemia virus receptor. J Virol. 1994; 68:626–631. [PubMed: 8289366]

Ellis RJ, Rosario D, Clifford DB, et al. Continued high prevalence and adverse clinical impact of human immunodeficiency virusâ€“associated sensory neuropathy in the era of combination antiretroviral therapy: The charter study. Archives of Neurology. 67:552–558. [PubMed: 20457954]

Ellis RJ, Rosario D, Clifford DB, McArthur JC, Simpson D, Alexander T, Gelman BB, Vaida F, Collier A, Marra CM, Ances B, Atkinson JH, Dworkin RH, Morgello S, Grant I. Continued high prevalence and adverse clinical impact of human immunodeficiency virusâ€“associated sensory neuropathy in the era of combination antiretroviral therapy: the CHARTER Study. Arch Neurol. 2010; 67:552–558. [PubMed: 20457954]

Emori Y, Ikeda T, Ohashi T, Masuda T, Kurimoto T, Takei M, Kannagi M. Inhibition of human immunodeficiency virus type 1 replication by Z-100, an immunomodulator extracted from human-type tubercle bacilli, in macrophages. J Gen Virol. 2004; 85:2603–2613. [PubMed: 15302954]

Ganor Y, Drillet-Dangeard AS, Lopalco L, Tudor D, Tambussi G, Delongchamps NB, Zerbib M, Bomsel M. Calcitonin gene-related peptide inhibits Langerhans cell-mediated HIV-1 transmission. J Exp Med. 2013; 210:2161–2170. [PubMed: 24081951]

Gardell LR, Vanderah TW, Gardell SE, Wang R, Ossipov MH, Lai J, Porreca F. Enhanced evoked excitatory transmitter release in experimental neuropathy requires descending facilitation. J Neurosci. 2003; 23:8370–8379. [PubMed: 12967999]

Giese NA, Giese T, Morse HC 3rd. Murine AIDS is an antigen-driven disease: requirements for major histocompatibility complex class II expression and CD4+ T cells. J. Virol. 1994; 68:5819–5824. [PubMed: 7914549]

Herzberg U, Sagen J. Peripheral nerve exposure to HIV viral envelope protein gp120 induces neuropathic pain and spinal gliosis. J Neuroimmunol. 2001; 116:29–39. [PubMed: 11311327]

Hewitt DJ, McDonald M, Portenoy RK, Rosenfeld B, Passik S, Breitbart W. Pain syndromes and etiologies in ambulatory AIDS patients. Pain. 1997; 70:117–123. [PubMed: 9150284]

Jolicoeur P. Murine acquired immunodeficiency syndrome (MAIDS): an animal model to study the AIDS pathogenesis. FASEB J. 1991; 5:2398–2405. [PubMed: 2065888]

Kraft-Terry SD, Buch SJ, Fox HS, Gendelman HE. A coat of many colors: neuroimmune crosstalk in human immunodeficiency virus infection. Neuron. 2009; 64:133–145. [PubMed: 19840555]

Kramer-Hammerle S, Rothenaigner I, Wolff H, Bell JE, Brack-Werner R. Cells of the central nervous system as targets and reservoirs of the human immunodeficiency virus. Virus Res. 2005; 111:194–213. [PubMed: 15885841]

Kustova Y, Espey MG, Sung EG, Morse D, Sei Y, Basile AS. Evidence of neuronal degeneration in C57B1/6 mice infected with the LP-BM5 leukemia retrovirus mixture. Mol Chem Neuropathol. 1998; 35:39–59. [PubMed: 10343970]

Kustova Y, Sei Y, Goping G, Basile AS. Gliosis in the LP-BM5 murine leukemia virus-infected mouse: an animal model of retrovirus-induced dementia. Brain Res. 1996; 742:271–282. [PubMed: 9117405]

Lee SE, Kim JH. Involvement of substance P and calcitonin gene-related peptide in development and maintenance of neuropathic pain from spinal nerve injury model of rat. Neurosci Res. 2007; 58:245–249. [PubMed: 17428562]

Liang M. Integrative pathway knowledge bases as a tool for systems molecular medicine. Physiol Genomics. 2007; 30:209–212. [PubMed: 17488890]

Malon JT, Maddula S, Bell H, Cao L. Involvement of calcitonin gene-related peptide and CCL2 production in CD40-mediated behavioral hypersensitivity in a model of neuropathic pain. Neuron Glia Biol. 2011; 7:117–128. [PubMed: 22377050]

Mayer AM, Hall M, Fay MJ, Lamar P, Pearson C, Prozialeck WC, Lehmann VK, Jacobson PB, Romanic AM, Uz T, Manev H. Effect of a short-term in vitro exposure to the marine toxin domoic acid on viability, tumor necrosis factor-alpha, matrix metalloproteinase-9 and superoxide anion release by rat neonatal microglia. BMC Pharmacol. 2001; 1:7. [PubMed: 11686853]

Mikami N, Sueda K, Ogitani Y, Otani I, Takatsuji M, Wada Y, Watanabe K, Yoshikawa R, Nishioka S, Hashimoto N, Miyagi Y, Fukada S, Yamamoto H, Tsujikawa K. Calcitonin Gene-Related Peptide Regulates Type IV Hypersensitivity through Dendritic Cell Functions. PLoS One. 2014; 9:e86367. [PubMed: 24466057]

Miller RG. Neuromuscular complications of human immunodeficiency virus infection and antiretroviral therapy. West J Med. 1994; 160:447–452. [PubMed: 8048229]

Millet I, Phillips RJ, Sherwin RS, Ghosh S, Voll RE, Flavell RA, Vignery A, Rincon M. Inhibition of NF-kappaB activity and enhancement of apoptosis by the neuropeptide calcitonin gene-related peptide. J Biol Chem. 2000; 275:15114–15121. [PubMed: 10809748]

Milligan ED, Mehmert KK, Hinde JL, Harvey LO, Martin D, Tracey KJ, Maier SF, Watkins LR. Thermal hyperalgesia and mechanical allodynia produced by intrathecal administration of the human immunodeficiency virus-1 (HIV-1) envelope glycoprotein, gp120. Brain Res. 2000; 861:105–116. [PubMed: 10751570]

Moreno-Fernandez ME, Rueda CM, Velilla PA, Rugeles MT, Chougnet CA. cAMP during HIV infection: friend or foe? AIDS Res Hum Retroviruses. 2012; 28:49–53. [PubMed: 21916808]

Moreno MJ, Terron JA, Stanimirovic DB, Doods H, Hamel E. Characterization of calcitonin gene-related peptide (CGRP) receptors and their receptor-activity-modifying proteins (RAMPs) in human brain microvascular and astroglial cells in culture. Neuropharmacology. 2002; 42:270–280. [PubMed: 11804624]

Narasipura SD, Kim S, Al-Harthi L. Epigenetic Regulation of HIV-1 Latency in Astrocytes. J Virol. 2014; 88:3031–3038. [PubMed: 24352441]

Ojeda D, Lopez-Costa JJ, Sede M, Lopez EM, Berria MI, Quarleri J. Increased in vitro glial fibrillary acidic protein expression, telomerase activity, and telomere length after productive human immunodeficiency virus-1 infection in murine astrocytes. J Neurosci Res. 2014; 92:267–274. [PubMed: 24254728]

Parameswaran N, Disa J, Spielman WS, Brooks DP, Nambi P, Aiyar N. Activation of multiple mitogen-activated protein kinases by recombinant calcitonin gene-related peptide receptor. Eur J Pharmacol. 2000; 389:125–130. [PubMed: 10688975]

Priller J, Haas CA, Reddington M, Kreutzberg GW. Calcitonin gene-related peptide and ATP induce immediate early gene expression in cultured rat microglial cells. Glia. 1995; 15:447–457. [PubMed: 8926038]

Rowe WP, Pugh WE, Hartley JW. Plaque assay techniques for murine leukemia viruses. Virology. 1970; 42:1136–1139. [PubMed: 4099080]

Sei Y, Kustova Y, Li Y, Morse HC 3rd, Skolnick P, Basile AS. The encephalopathy associated with murine acquired immunodeficiency syndrome. Ann N Y Acad Sci. 1998; 840:822–834. [PubMed: 9629308]

Sei Y, Makino M, Vitkovic L, Chattopadhyay SK, Hartley JW, Arora PK. Central nervous system infection in a murine retrovirus-induced immunodeficiency syndrome. J Neuroimmunol. 1992; 37:131–140. [PubMed: 1548376]

Simpson DM, Haidich A-B, Schifitto G, Yiannoutsos CT, Geraci AP, McArthur JC, Katzenstein DA, the, A.s.t. Severity of HIV-associated neuropathy is associated with plasma HIV-1 RNA levels. AIDS. 2002; 16:407–412. [PubMed: 11834952]

Suzumura A, Sawada M, Makino M, Takayanagi T. Propentofylline inhibits production of TNFalpha and infection of LP-BM5 murine leukemia virus in glial cells. J Neurovirol. 1998; 4:553–559. [PubMed: 9839653]

Wallace VCJ, Blackbeard J, Pheby T, Segerdahl AR, Davies M, Hasnie F, Hall S, McMahon SB, Rice ASC. Pharmacological, behavioural and mechanistic analysis of HIV-1 gp120 induced painful neuropathy. PAIN. 2007; 133:47–63. [PubMed: 17433546]

Wang H, Kavanaugh MP, North RA, Kabat D. Cell-surface receptor for ecotropic murine retroviruses is a basic amino-acid transporter. Nature. 1991; 352:729–731. [PubMed: 1908564]

Wang H, Klamo E, Kuhmann SE, Kozak SL, Kavanaugh MP, Kabat D. Modulation of ecotropic murine retroviruses by N-linked glycosylation of the cell surface receptor/amino acid transporter. J Virol. 1996; 70:6884–6891. [PubMed: 8794331]

Zaritsky LA, Gama L, Clements JE. Canonical type I IFN signaling in simian immunodeficiency virus-infected macrophages is disrupted by astrocyte-secreted CCL2. J Immunol. 2012; 188:3876–3885. [PubMed: 22407919]

Zhang JS, Tan YR, Xiang Y, Luo ZQ, Qin XQ. Regulatory peptides modulate adhesion of polymorphonuclear leukocytes to bronchial epithelial cells through regulation of interleukins, ICAM-1 and NF-kappaB/IkappaB. Acta Biochim Biophys Sin (Shanghai). 2006; 38:119–128. [PubMed: 16474903]

Zheng LF, Wang R, Xu YZ, Yi XN, Zhang JW, Zeng ZC. Calcitonin gene-related peptide dynamics in rat dorsal root ganglia and spinal cord following different sciatic nerve injuries. Brain Res. 2008; 1187:20–32. [PubMed: 18035338]

Zheng W, Ouyang H, Zheng X, Liu S, Mata M, Fink DJ, Hao S. Glial TNFalpha in the spinal cord regulates neuropathic pain induced by HIV gp120 application in rats. Mol Pain. 2011; 7:40. [PubMed: 21599974]

Zybarth G, Reiling N, Schmidtmayerova H, Sherry B, Bukrinsky M. Activation-induced resistance of human macrophages to HIV-1 infection in vitro. J Immunol. 1999; 162:400–406. [PubMed: 9886413]

## Highlights

- There was a significant upregulation of spinal cord CGRP in Murine AIDS infection.
- CGRP reduced viral load in mixed glia in a microglial content-dependent manner.
- CGRP's anti-retroviral effect requires interaction between CGRP and host cell.

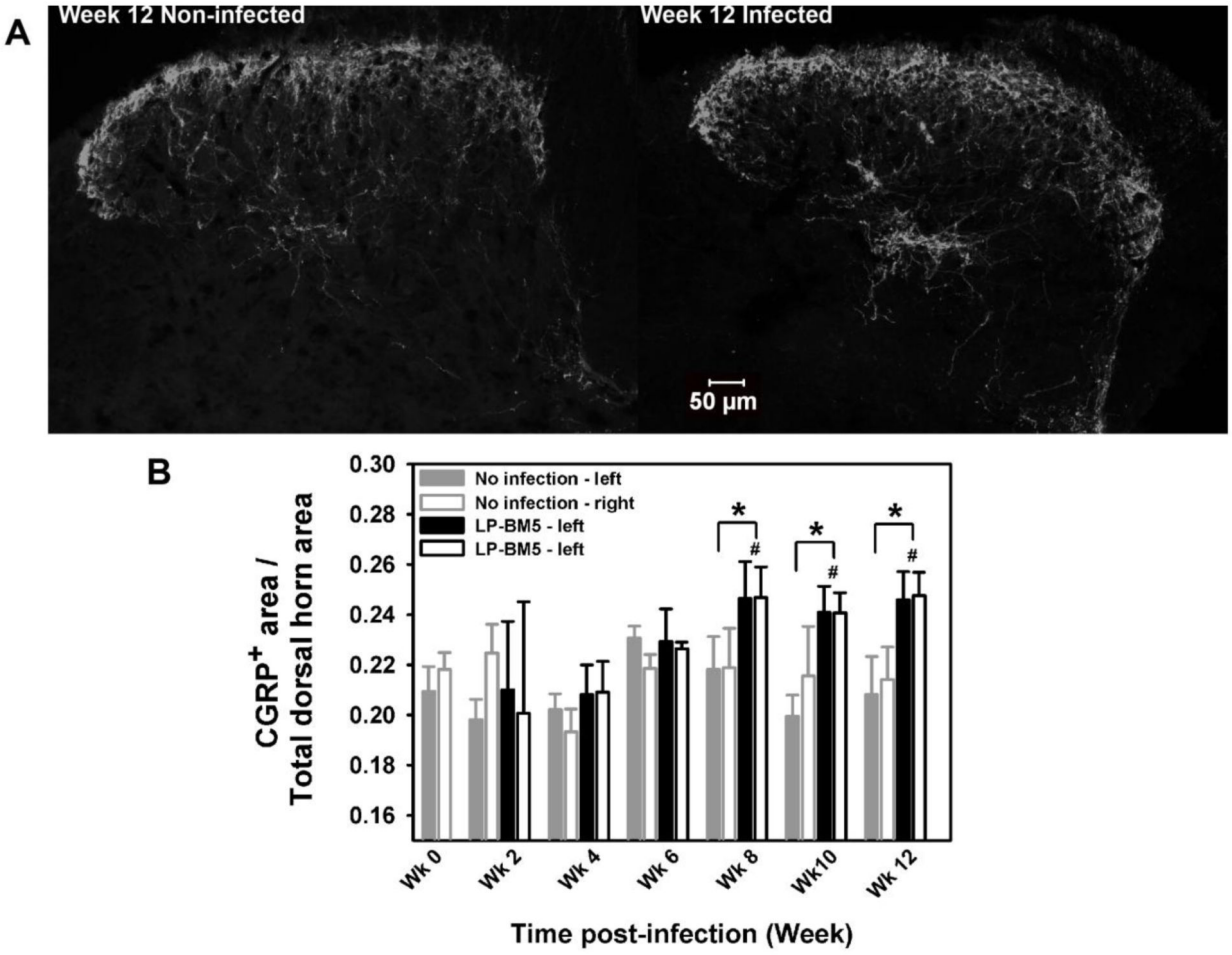


**Figure 1. Spinal cord CGRP expression following LP-BM5 infection in B6 mice**

Adult B6 mice were randomly assigned into non-infected and LP-BM5 infected groups ($5\times10^4$ PFU per mouse, i.p.). Lumbar spinal cords were collected before infection and 2, 4, 6, 8, 10, and 12 weeks post-infection and then processed for IHC to examine CGRP expression. Representative images of the right side of lumbar spinal cord dorsal horn region from non-infected (A) and infected (B) mice 12 weeks post-infection are shown here (10 ×, scale bar = 50 μm). CGRP expression was quantified as described in the Materials and Methods. Quantitative data are shown in C (Mean ± SEM, n = 4). Paired *t*-test was first performed to determine the differences between the left and right sides. And then two-way ANOVA was performed using time and infection as factors followed by the SNK *post-hoc* test. * indicates $p < 0.05$ between the designated treatment groups regardless of the side (left or right). # indicates $p < 0.05$ between the designated group and the corresponding week 0 control group regardless of the side (left or right).

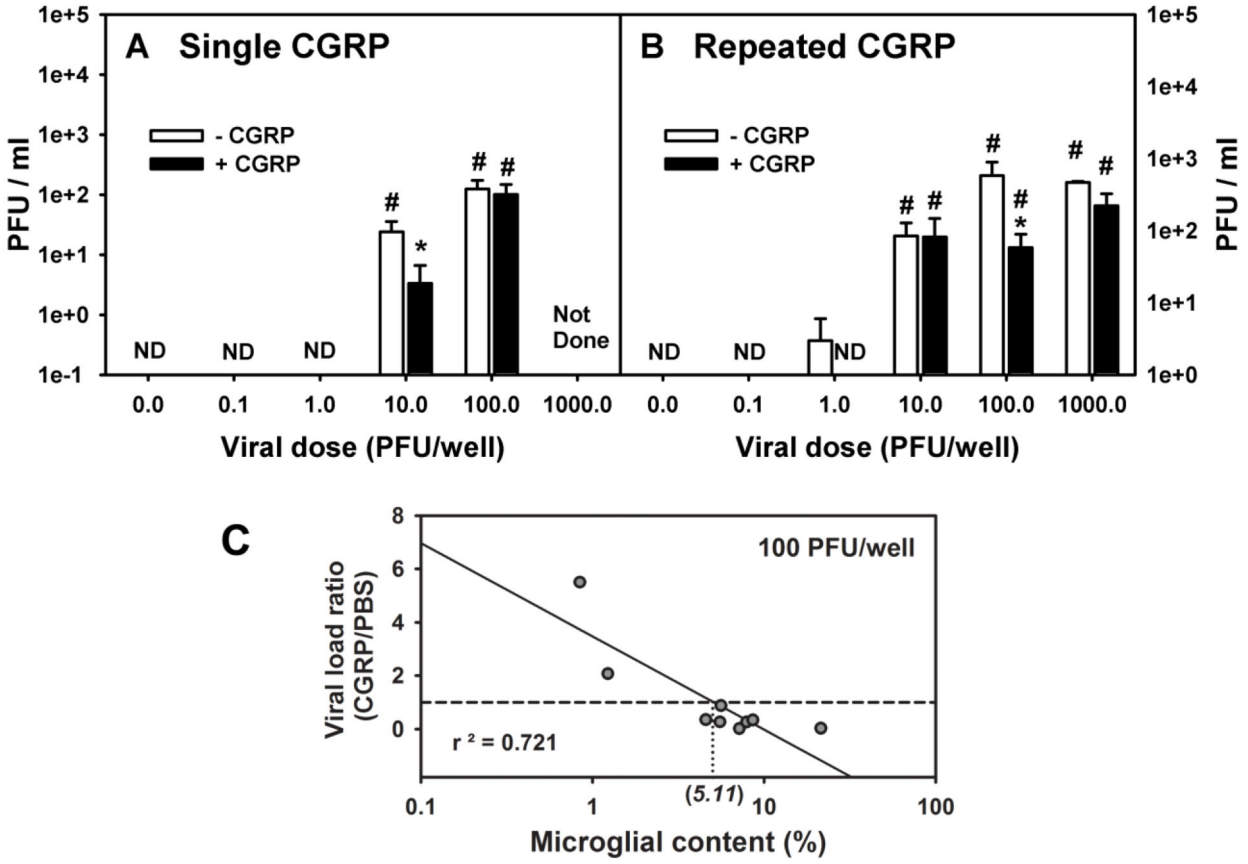


**Figure 2. Effects of CGRP on viral loads in LP-BM5 infected mixed glial cells**

Adult spinal cord mixed glial cultures were prepared as described in the Materials and Methods. Cells were infected with various doses of LP-BM5 ± CGRP (1000 ng/ml) treatment (either once (A, n = 4) or repeatedly (B, n = 4-6 for all groups except n = 2 for LP-BM5 at 1000 PFU/well)). Viral loads were determined at day 7 post-infection via XC plaque assay. All data are presented as Mean ± SEM. For data with each type of CGRP treatment, two-way ANOVA was performed using viral dose and CGRP treatment as factors followed by the SNK *post-hoc* test. * indicates $p < 0.05$ between the designated group and the corresponding non-CGRP treated group with the same dose of viral infection. # indicates $p < 0.05$ between the designated group and the corresponding non-infected control group. In C, data collected from cultures treated with 100 PFU/well of LP-BM5 ± repeated treatment of CGRP were used to generate the dot plot: viral loads with CGRP treatment/viral loads without CGRP treatment vs. microglial content within each set of culture. Dash line (ratio between viral loads = 1) indicates no CGRP effects. The microglial content (5.11) at which the viral load ratio equals 1 is marked on the x-axis. The linear regression curve (solid line) and $r^2$ value are shown within the graph.

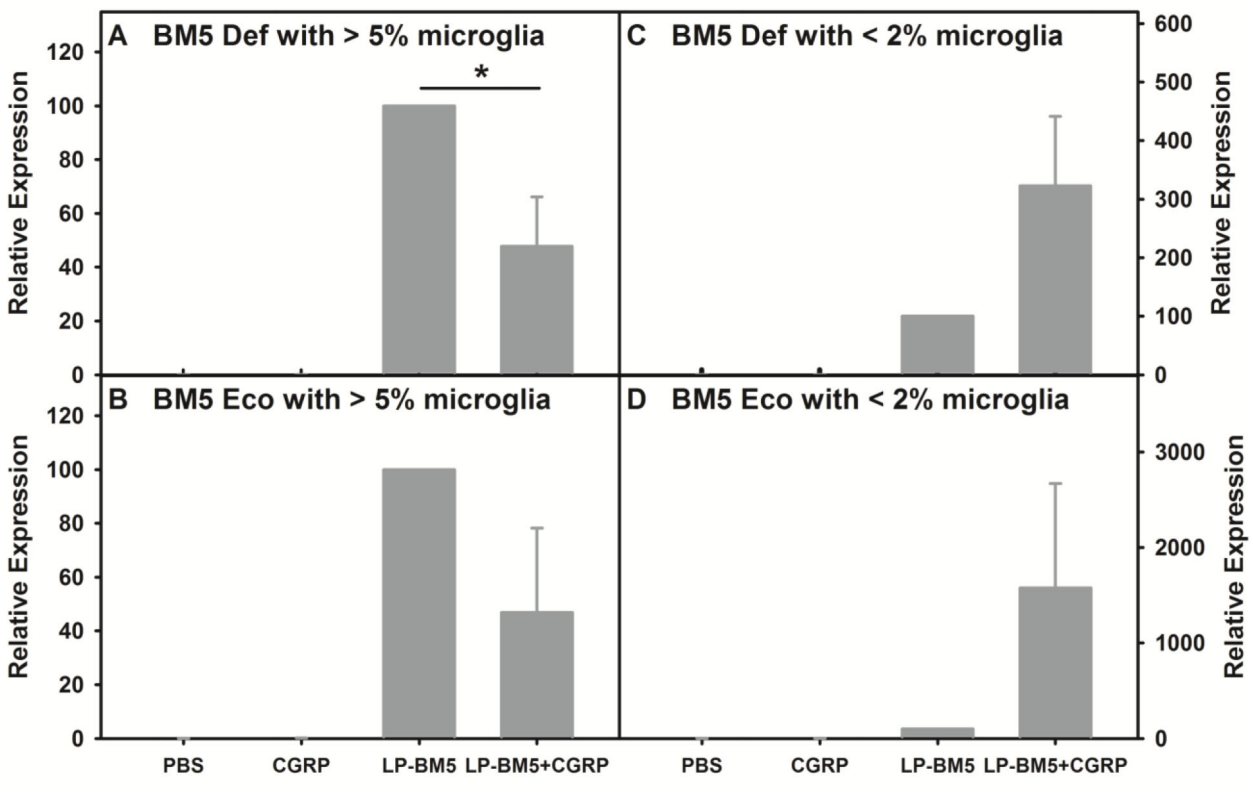


**Figure 3. Effects of CGRP on viral loads in LP-BM5 infected microglia-rich and microglia-lacking mixed glial cells**

Adult spinal cord mixed glial cultures were prepared as described in the Materials and Methods. Cells were infected with various doses of LP-BM5 (100 PFU/well) ± repeated CGRP (1000 ng/ml) treatment as described in Figure 2. Viral loads were determined at day 7 post-infection via qRT-PCR. The gag genes of both of the BM5def and BM5eco were examined. Data are presented separately based on the microglial content within the mixed glia at the time of treatment. Cultures with microglial content greater than 5% are defined as microglia-rich cultures (A and B, n = 5) and cultures with less than 2% of microglia are defined as microglia-lacking cultures (C and D, n = 3). Within each set of experiments, LP-BM5 infected group was set at 100% and all other groups were normalized to LP-BM5 infected group. Note that the values for non-infected groups, “PBS” and “CGRP” groups are either 0 or extremely low, thus no group bars for these groups are seen in each graph. All data are presented as Mean ± SEM. One-way ANOVA was performed followed by the SNK *post-hoc* test. Within each graph, values of either infected groups are significantly different from that of either non-infected groups. * indicates $p < 0.05$ between the designated groups.

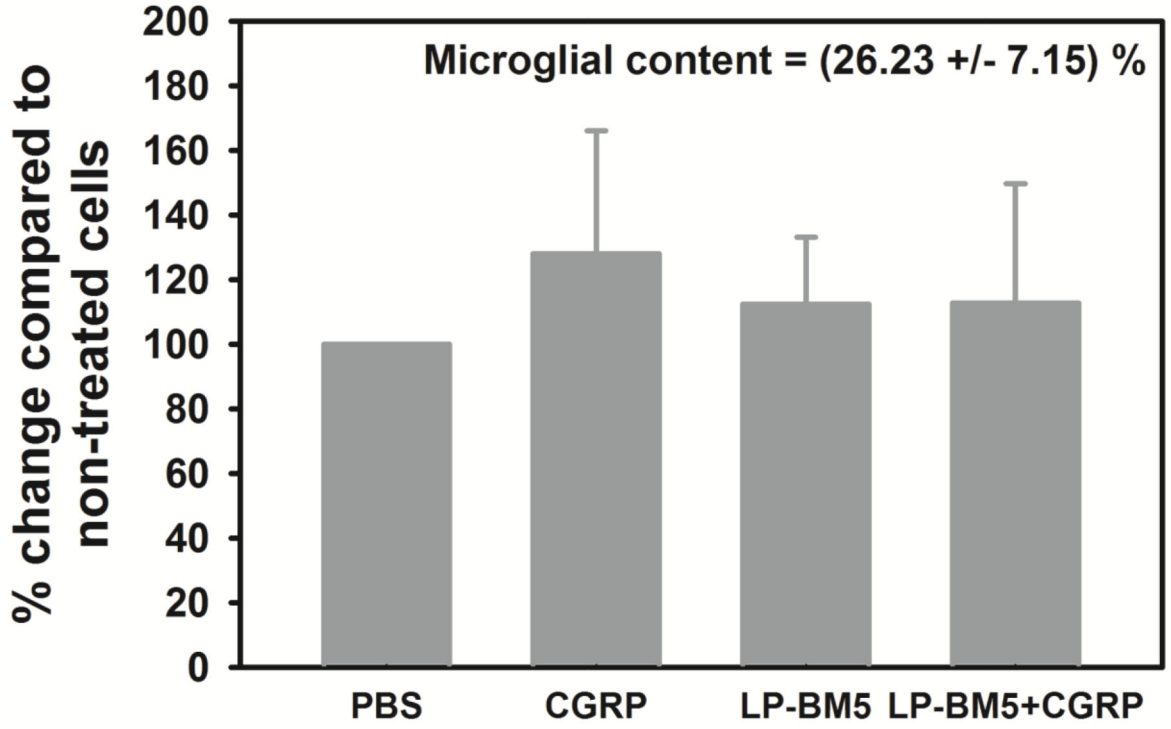


**Figure 4. Cell viability following LP-BM5 ± CGRP treatment**

Microglia-rich adult spinal cord mixed glial cultures were prepared as described in the Materials and Methods. Cells were infected with 100 PFU/well of LP-BM5 ± repeated CGRP treatment (1000 ng/ml). Cell viability was measured via MTT assay at 7 days post-infection. Within each experiment, the average OD570 values for PBS group was set as 100% and all other treatment groups were normalized to the PBS group. Data are presented as Mean ± SEM (n = 3). One way ANOVA was performed and no significant changes in cell viability following treatment were found.

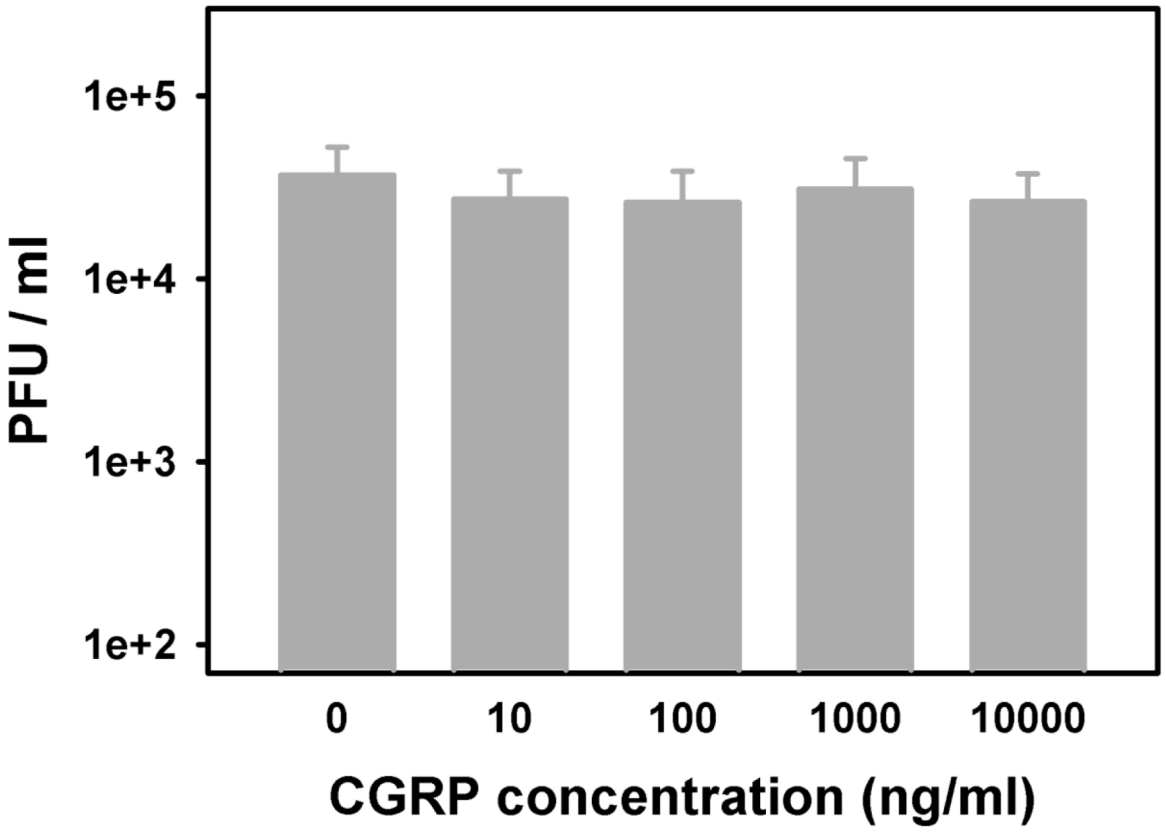


**Figure 5. Direct effects of CGRP on LP-BM5 virus**

LP-BM5 ($10^4$ PFU/ml) were incubated with CGRP at various doses in PBS at 37°C for 1 hour. At the end of incubation, the viral load of each viral suspension was determined via XC plaque assay. Viral counts are presented as Mean ± SEM (n = 3). One way ANOVA was performed and no significant differences were found between any groups.

## Table 1

**Production of selected cytokines/chemokines by mixed glia 7 days following LP-BM5 infection (100 PFU/well) with and without repeated CGRP (1000 ng/ml) treatment**

| Treatment CGRP(ng/ml)/LP-BM5 (PFU/well) | 0/0 | 1000/0 | 0/100 | 1000/100 |
|---|---|---|---|---|
| **IL-6 (mean ± SEM)** | 378.08 ± 178.44 | 326.78 ± 114.58 | 300.19 ± 129.29 | 340.31 ± 104.51 |
| **TNF-alpha (mean ± SEM)** | 10.93 ± 2.65 | 8.27 ± 2.03 | 8.44 ± 3.18 | 5.76 ± 2.50 |
| **IL-12/IL-23 p40 (mean ± SEM)** | 37.88 ± 13.47 | 40.47 ± 13.72 | 22.35 ± 6.78 | 19.57 ± 6.22 |
| **CCL2 (mean ± SEM)** | 12714.11 ± 7344.53 | 11210.38 ± 5855.77 | 13172.59 ± 6278.97 | 10025.88 ± 4255.77 |